Bremsstrahlung effects in energetic particle detectors

M. Tuszewski, T. E. Cayton, J. C. Ingraham, and R. M. Kippen

Los Alamos National Laboratory, Los Alamos, New Mexico, USA

[1] The energetic charged particles of the Earth's magnetosphere are routinely detected by solid-state satellite instruments. Quantitative data are increasingly required for engineering dose calculations and for space weather science. However, the design of some energetic particle detectors can be severely constrained. Background effects must be accurately modeled in such cases to extract quantitative information. In particular, bremsstrahlung radiation from electrons impacting the detector and the satellite often dominates the background noise. Numerical tools are presented here to calculate total bremsstrahlung effects in energetic electron detectors. The calculations are illustrated for the low-energy particle detector of current Global Positioning System satellites. INDEX TERMS: 2720 Magnetospheric Physics: Energetic particles, trapped; 2732 Magnetospheric Physics: Magnetosphere interactions with satellites and rings; 2794 Magnetospheric Physics: Instruments and techniques; KEYWORDS: bremsstrahlung, energetic particle detector, satellite

1. Introduction

[2] The energetic (30 keV to 10 MeV) charged particles of the Earth's radiation belts are detected by many solid-state satellite instruments. A quantitative determination of the particle fluxes and of their energy spectra is becoming increasingly important. The total dose of penetrating charged particles must be known for electronics design and fault analysis and to estimate damage to satellite electronics. The charged particle data of several satellites must be compared in magnetospheric science and space weather studies.

[3] Quantitative particle data imply accurate instrumental responses. However, the responses of energetic electron detectors can be greatly complicated by angular scattering and by bremsstrahlung radiation [Vampola, 1998]. The latter process is often the dominant background effect when the energetic (>1 MeV) electron populations are large. Cosmic rays and solar protons can also yield significant background noise in some cases.

[4] Bremsstrahlung effects in energetic particle detectors can be minimized with shielding and coincidence schemes. Some examples are the Magnetic Electron Spectrometer [Vampola et al., 1992], the Proton and Electron Telescope [Cook et al., 1993], the High-Sensitivity Telescope [Blake et al., 1995], and the Energetic Particle Detector [Jun et al., 2002].

[5] However, substantial bremsstrahlung effects are likely when design constraints do not permit noise reduction techniques. This is the case for the electron detectors of the Global Positioning System (GPS) satellites, which weigh less than 0.25 kg, have limited electronics, and must routinely sample high electron fluxes in the outer radiation belt. The GPS design constraints are detailed in section 2. The energetic electron detectors of future constellation missions, crucial to benchmark future space weather mod-els, may also be necessarily small [Angelopoulos and Panetta, 1998].

[6] Instrument designers should always strive to reduce background effects as much as possible. However, detailed response calculations can be very valuable for cases where sufficient background reduction is not possible. The present research focuses on cases where bremsstrahlung radiation is the dominant background effect. We show that quantitative information can still be obtained in such cases.

[7] Beam calibrations [Rosen and Sanders, 1968] and Monte Carlo calculations [Drake et al., 1993; Jun et al., 2002] are often used to analyze the instrumental responses. However, such expensive tools are usually only applied to the detector head. As will be shown in sections 3 and 4, a complete analysis must also include the detector box and many of the satellite structures. Such complete calculations have been performed to quantify spacecraft radiation doses [Fan et al., 1996] and to evaluate the background of gamma-ray telescopes [Dean et al., 2003].

[8] In spite of increasingly powerful computers, complete Monte Carlo calculations of electron detector responses are still prohibitively expensive. This is because the energy spectra must be resolved in sensor volumes that are very small (<1 mL) compared with the spacecraft volume. This situation contrasts with dose calculations that do not resolve the energy spectra and with background calculations in large (several liters) gamma-ray detectors.

[9] The analytical probability (AP) formalism is a relatively inexpensive numerical technique that can be used to analyze instrumental responses [Tuszewski et al., 2002]. Numerous benchmarks with Monte Carlo N-particle (MCNP) simulations [Briesmeister, 1986] have demonstrated that AP calculations can provide reasonably accurate (50% uncertainties) estimates of bremsstrahlung
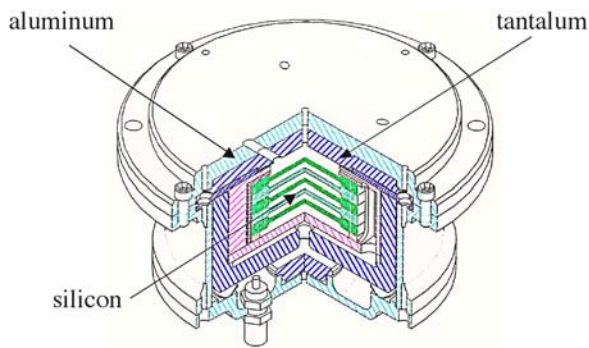
Figure 1. Sketch of the low-energy particle (LEP) detector head.

effects. Even more accurate instrumental responses can be obtained by combining Monte Carlo calculations of the detector head with AP calculations of the detector box and of the satellite. Such complete calculations are presented here for the low-energy particle (LEP) detector of Block IIR GPS satellites.

[10] The paper is organized as follows. The LEP detector, the combined X-ray and dosimeter (CXD) detector box, and the GPS satellite are described in section 2. The calculations of total LEP electron responses are presented in section 3. Typical LEP electron count rates are analyzed in section 4, assuming total and partial instrumental responses. The results are discussed in section 5, and some conclusions are offered in section 6.

2. LEP Detector

[11] The LEP detectors, developed by Los Alamos National Laboratory, are beginning to be deployed on GPS IIR satellites. Two instruments are already in orbit, and seven additional LEP detectors will be flown in the next few years. The GPS satellites have inclined (55°) circular orbits 20,000 km above the Earth's surface. With orbital periods of about 12 hours, the LEP detectors sample every 3 hours the energetic charged particle environment (L shell values from 4.2 to about 25).

[12] The LEP detector head is sketched in Figure 1. The detector consists of five 0.5-mm-thick silicon wafers (manufactured by Canberra Industries) connected electrically in parallel. The LEP detector responds to electrons in the range $0.14-70$ MeV and to protons in the range $6-50$ MeV. The detector is surrounded by a cylindrical shield that includes 3 mm of aluminum outside of 3 mm of tantalum. Four collimating channels (one at 0° and three at 45°) through the top shield provide particle sampling over a solid angle of about 110°. A 0.05-mm-thick aluminum filter defines the lower energy thresholds.

[13] The incident charged particles deposit their energy in the silicon detector layers, creating charge pulses of a few microseconds that are shaped, amplified, and analyzed by suitable electronics. The electron signals are sorted in five differential channels, with electronic thresholds corresponding to 0.075, 0.18, 0.36, 0.72, and 1.2 MeV deposited energies. The proton signals are sorted in two channels, with electronic thresholds of approximately 5 and 10 MeV. The upper deposited energy for the last electron channel coincides with the lower proton threshold.

[14] Bremsstrahlung photons can also deposit energy in the LEP detector, in the same range as the incident electrons. Hence the photons may also be counted as electrons by the instrument logic. In order to derive the true electron fluxes, the deposited energy spectra of monoenergetic electrons incident on the detector, the CXD box, and the spacecraft must be modeled. These spectra include electron and bremsstrahlung photon contributions. Many different incident electron energies are considered, in separate calculations, to obtain the instrumental responses.

[15] The LEP detector is part of the combined X-ray and dosimeter (CXD) package. The detector head is mounted near a corner of the CXD box, as sketched in Figure 2. The aluminum walls of the box ($0.11 \times 0.2 \times 0.28$ m) are 5 mm thick. The box is mounted near a corner of the Earth-facing surface of the GPS satellite. The satellite is rectangular in shape ($1.5 \times 1.9 \times 1.5$ m). The satellite surfaces are made of a honeycomb aluminum structure. The details of the inside of the satellite, of the W sensor antennas, and of the solar panels are not necessary for the present study.

[16] The LEP detector design is severely constrained. The detector head, including shielding, must weigh less than 0.25 kg because the entire CXD box is limited to 8 kg and includes 11 separate instruments. The stack of five silicon wafers is necessary because of the CXD 250 V maximum voltage. A coincidence scheme to reduce background effects could not be implemented in the small LEP electronics card. The number and size of the collimators are limited by the anticipated maximum count rates and by the estimated 15-year radiation damage to the silicon detectors.

3. LEP Responses

[17] The LEP count rates are related to the incident particle fluxes through instrumental response functions. Those responses are determined as functions of the incident electron energy E as follows. First, MCNP [*Briesmeister*, 1986] and AP [*Tuszewski et al.*, 2002] calculations of the detector head are performed with and without a 60-mm-diameter back hemisphere to approximate the box and the satellite. Second, AP bremsstrahlung calculations are made with realistic CXD box and GPS satellite geometries. The surfaces are divided into about 2000 elements, and the contributions of all elements are summed. Third, the ratios of AP calculations with the actual geometries to those with the hemispherical back model are determined. Finally, the LEP total responses are obtained by adding the MCNP detector head responses to the MCNP responses of the back hemisphere multiplied by the above AP ratios.

[18] The AP calculations are useful to separate the respective contributions of different processes. For example, the total integral response of the first LEP electron channel is shown in Figure 3 with the upper solid curve. The geometrical integral response, defined by the four
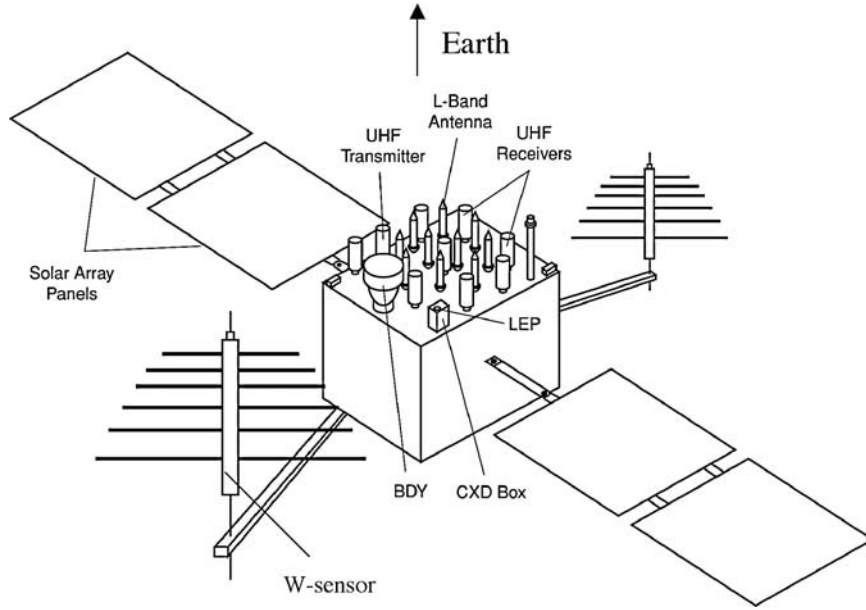
Figure 2. Sketch of the GPS Block IIR satellite.

collimators and by the aluminum filter, is shown in Figure 3 with the lower solid curve. The filter somewhat modifies the step function−like integral geometrical response, owing to electron transmission and backscattering. Forward scattering on the collimator walls is the main cause of the difference between total and geometrical responses for $E < 1$ MeV.

[19] The bremsstrahlung contribution to the total detector response is shown by the dashed curve in Figure 3. Bremsstrahlung is clearly an important process, since it increases the detector response by several orders of magnitude for large values of E. Analysis, too lengthy to be detailed here, shows that the bremsstrahlung response can be approximated by

$$G \sim (R/X)\left(\int d\sigma/r^2\right)(\mu_d L_d)(A_d h/3). \qquad (1)$$

The first term of equation (1) is the ratio of the electron range R to the e-folding radiation length X [Grupen, 1996]. The second integral term includes all surface elements $d\sigma$, and r is the distance between a given element and the detector. The third term, $\mu_d L_d \ll 1$, accounts for photon absorption in the detector thickness L_d. The fourth term includes the detector area A_d, a factor of 3 from angular averages, and h, a normalized spectrum for photons that reach the detector. The dimensionless quantity h is of order unity, and it depends on the incident electron energy E, on the electronic threshold E_t, and on photon attenuation up to the detector. For LEP, one can approximate

$$
\begin{aligned}
h(E, E_t) = &\left(1 + 2E_0/E + E_0 E_t/E^2\right)\log(E/E_t)\\
&- (1 - E_t/E)(1.5 + 3E_0/E - 0.5E_t/E),
\end{aligned} \qquad (2)
$$

where E_0 is the electron rest mass. Equation (2) is valid for 0.3 MeV $\leq E_t \leq E$, where the lower limit comes from a sharp boundary photon attenuation model. Outside of this range, $h = h(E, 0.3)$ for $E_t < 0.3$ MeV and $h = 0$ for $E_t > E$.

[20] Useful scaling laws can be obtained from equations (1) and (2). One can approximate $R/X \sim 4.5 \times 10^{-4} Z E^{1.65}$, where Z is the surface atomic number. For a given E value, $G \sim h$ decreases as E_t increases. For a given E_t value, $G \sim A_d L_d E^\alpha \int Z d\sigma/r^2$, where $\alpha \sim 2$ to 3 includes the $h(E)$ dependence. The bremsstrahlung response is proportional to the detector volume and increases strongly with E as shown in Figure 3.

[21] The surfaces exposed to incident electrons contribute as $\int Z d\sigma/r^2$, where the appropriate Z values must be used for each surface element. The bremsstrahlung contributions of the aluminum LEP detector head, CXD box,
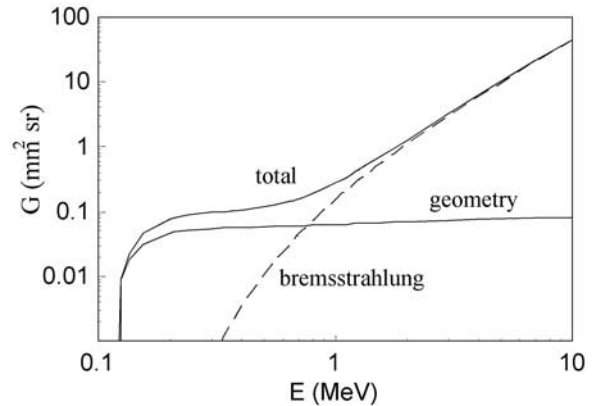

Figure 3. Integral responses of the first LEP electron channel as functions of incident electron energy.
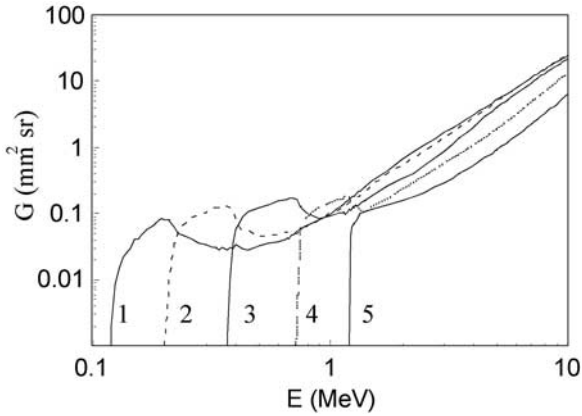
Figure 4. Differential responses of the five LEP channels as functions of incident electron energy.

and GPS satellite scale as their $\int d\sigma/r^2$ values of 7.5, 16.1, and 11.6, respectively. The substantial box and satellite contributions must be included in the response calculations.

[22] Approximate bremsstrahlung responses can be obtained from equations (1) and (2). One calculates $G \sim 0.15$ mm^2 sr for the first LEP electron channel and for $E = 1$ MeV, with $A_d = 150$ mm^2, $\mu_d L_d \sim 0.025$ for the 2.5-mm-thick silicon detector, $Z = 13$, $\int d\sigma/r^2 = 35.2$ for all surfaces, and $h(1, 0.075) \sim 0.6$. The approximate value of G coincides with that obtained numerically with the full AP formalism (dashed curve in Figure 3).

4. LEP Data Example

[23] The count rates C_i (s^{-1}) of the five ($i = 1$ to 5) LEP electron channels are related to the electron flux $j(E)$ (mm^{-2} s^{-1} sr^{-1} MeV^{-1}) through differential responses G_i (mm^2 sr) as

$$C_i = \int j(E)G_i(E)dE, \tag{3}$$

where the integral is evaluated over all incident energies. The differential responses G_i are obtained by subtracting integral total responses, such as in Figure 3, with successive thresholds.

[24] The LEP differential responses, from combined MCNP and AP calculations, are shown in Figure 4. Different line styles are used to avoid confusion. The differential responses would be approximately constant (in the range $0.06-0.08$ mm^2 sr) in between successive electronic thresholds if geometry was the only process. The actual responses look more like integral responses. The large increases in each channel for $E > 1$ MeV are due to bremsstrahlung radiation.

[25] Given the count rates C_i and the responses G_i, the electron flux $j(E)$ can be estimated from equation (3). Simple conversion factors cannot be defined, and equation (3) must be numerically inverted. A forward approach to the inversion problem is used here. The phase

space density $j(E)/(mv)^2$ is modeled as $AE^B \exp(-E/C)$. The three parameters A, B, and C, which provide the best match between measured and calculated count rates, are then determined by a least squares numerical procedure.

[26] A set of representative LEP count rates is shown with solid circles in Figure 5a. These rates were measured on 7 July 2001, during a 4-min time interval around 2240 UT. The GPS IIR satellite (NavStar 54) was near the magnetic equator of the Earth (L $\sim$ 4.4), on the dusk side (1930 local time). The electron population, and hence the LEP count rates, were somewhat below average during this quiet period (the *Dst* magnitude was less than 50 nT during the previous month).

[27] The electron flux $j(E)$ calculated with the total responses of Figure 4 is shown with a solid curve in Figure 5b. This total flux is presumably the most accurate estimate of the real electron flux, given the LEP count rates. The fluxes calculated with detector only (dashed curve) and geometrical (dotted curve) responses are also included in Figure 5b. The calculated count rates of the three cases, joined with the respective line styles, are shown in Figure 5a. Significantly different electron fluxes are obtained, while fitting adequately the measured count rates, depending on the response estimates.

[28] The detector flux corresponds to responses estimated with Monte Carlo simulations and/or experimental calibrations of only the detector head. The detector flux is much higher than the total flux for low E values because the detector responses neglect the box and satellite bremsstrahlung contributions that are significant for low
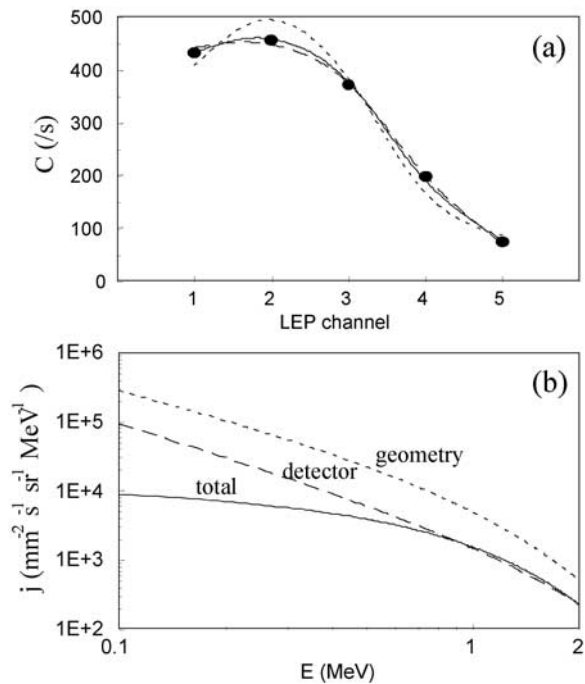

Figure 5. Example of LEP electron (a) count rates and (b) inferred fluxes. The curves correspond to total, detector only, and geometrical responses.

E_t values. Both fluxes are comparable for high E values because bremsstrahlung effects are reduced for channels with higher E_t values.

[29] The geometrical flux corresponds to the response of electrons passing through the collimators. The geometrical flux is larger than the detector flux by a factor of between 3 and 4 for low E values and by a factor of about 2 for high E values. Most of the discrepancy comes from electron forward scattering on the collimator walls and from detector head bremsstrahlung. The latter causes larger discrepancies for low E values, for reasons mentioned above.

[30] The best fit between calculated and measured counts is obtained with total responses, although the fit obtained with detector responses is nearly as good. The geometrical responses yield the worst fit, as can be seen in Figure 5a. More accurate total fluxes can be obtained by including the six high-energy electron channels of a separate CXD instrument. However, the fluxes calculated with 11 electron channels are qualitatively similar to those of Figure 5b. Hence the LEP data alone are sufficient to illustrate the sensitivity of the inferred electron flux to the various responses.

5. Discussion

[31] Bremsstrahlung radiation, from energetic electrons impacting the detector and the satellite structures, can be an important source of background noise for some satellite energetic particle detectors. Although the multistep bremsstrahlung process is very inefficient, it typically involves very large areas. Hence the bremsstrahlung photons can increase significantly the electron responses, as illustrated here with the LEP detector.

[32] Energetic particle detectors can be designed to minimize bremsstrahlung effects. Many such instruments have successfully measured energetic charged particles within the solar system. However, the design of some energetic charged particle detectors can be severely constrained. The detectors of current GPS satellites are one example. Future magnetospheric science and space weather missions may involve many miniature satellites, with necessarily small instruments.

[33] For a given detector design, the bremsstrahlung contributions to the instrumental responses are largest for (1) locations with high populations of energetic (>1 MeV) electrons, such as the outer radiation belt; (2) times when the electron energy distribution includes a substantial high-energy tail; and (3) instrument channels with low (<1 MeV) electronic thresholds. The latter reflects the fact that most bremsstrahlung photons are produced with low energies.

[34] Bremsstrahlung responses are difficult to determine because complete calculations must include the detector box and the satellite structures. Such calculations remain impractical with Monte Carlo techniques for very small solid-state detectors. It would take on the order of a trillion incident electrons to calculate the total LEP responses with the state-of-the-art Monte Carlo codes listed by *Dean et al.* [2003]. Hence we combine Monte Carlo and AP calcula-

tions to obtain the total detector responses. Adequate MCNP statistics already required a few 10^8 incident electrons for some incident electron energies.

[35] The AP and MCNP calculations were benchmarked against each other and against laboratory tests for special cases. First, the LEP instrument with and without a back hemisphere was modeled with both approaches. The results were in fair (<50%) agreement for all E values and for all channels. Second, a (0.1 × 0.1 m) strontium/yttrium beta source was placed against selected CXD box surfaces, and the LEP detector counts were accumulated over 4-min intervals. The measured counts were compared with AP and MCNP calculations, and good (<30%) agreement was obtained for all cases.

[36] In spite of the above benchmarks the calculated LEP total responses still have estimated uncertainties of about 50% because of several approximations made in the box and satellite contributions. Photon production involves the inside of the satellite for sufficiently high E values because of surface penetration by energetic electrons. This added complexity is neglected in the present AP calculations. The unknown electron pitch angle distribution also causes response uncertainties of typically $10-20\%$. The incident fluxes presumably vary on different surfaces, in proportions that change in time according to the unknown magnetic field orientation.

[37] Fortunately, it is not necessary to consider all the details of the box and of the satellite to obtain a reasonable estimate of the bremsstrahlung contributions. The exposed surface elements contribute approximately as the inverse square distance to the detector. Hence only the structures near the detector must be modeled accurately. Far away surfaces, such as solar panels and external antennas, are unimportant. The inverse square distance scaling also explains why the detector head, the box, and the satellite have comparable overall contributions in spite of vastly different surface areas.

[38] Specific calculations must be made for each energetic satellite detector, since details differ. The total responses of the burst detection dosimeter energetic electron detectors have similar bremsstrahlung contributions as those of LEP [*Tuszewski et al.*, 2002]. Calculations in progress suggest that bremsstrahlung is important for some of the electron channels of the Synchronous Orbit Particle Analyzer (SOPA) instrument [*Belian et al.*, 1992]. Bremsstrahlung photons also contaminate some of the SOPA proton channels with low energy thresholds. A similar contamination has been identified for the Medium-Energy Proton and Electron Detector [*Sauer*, 1978].

[39] Bremsstrahlung effects can be reduced by minimizing the detector volume, by optimizing the detector location on the box, and by using low-Z materials (beryllium or carbon composite) for some of the detector head and box surfaces. However, even combined, such modifications cannot typically reduce bremsstrahlung contributions by more than a factor of 2. Given the LEP design constraints, the most effective way to reduce bremsstrahlung effects may be to increase the number and/or diameter of the

collimators, at the expense of increased detector radiation damage and dead time losses.

[40] Past satellites were heavy, instrumentation resources were large, and computing capabilities were limited. Shielding and coincidence schemes were effective to reduce instrumental background effects. Now there is an increasing trend toward smaller satellites and reduced instrumental resources. Hardware solutions to reduce background effects may be impractical in many cases. However, computing capabilities continue to increase, enabling complete background calculations such as those presented here.

6. Conclusion

[41] Bremsstrahlung radiation can increase significantly the electron responses of some satellite energetic particle detectors. This is especially the case for small instruments sampling large populations of energetic electrons and measuring particles with energies in the range 0.1– 1 MeV. Bremsstrahlung calculations are complex because they involve satellite structures in addition to the detector. Numerical techniques are presented here that permit calculations of total instrumental responses. Such calculations are illustrated for the LEP detectors of current GPS satellites.

[42] Accurate instrumental responses are increasingly required for engineering dose estimates and for space weather science. The responses calculated in this paper have estimated uncertainties of about 50%. The computations are rapidly becoming easier to implement as insight is gained and as computer capabilities continue to increase. Those numerical tools promise a near-term quantitative analysis of the energetic particle data from satellite constellations such as GPS.

References

Angelopoulos, V., and P. V. Panetta (Eds.) (1998), *Science Closure and Enabling Technologies for Constellation Class Missions*, Univ. of Calif., Berkeley.

Belian, R. D., G. R. Gisler, T. E. Cayton, and R. Christensen (1992), High-Z energetic particles at geosynchronous orbit during the great solar proton event series of October 1989, *J. Geophys. Res.*, *97*, 16,897–16,906.

Blake, J. B., et al. (1995), CEPPAD: Comprehensive energetic particle and pitch angle distribution experiment on Polar, *Space Sci. Rev.*, *71*, 531–562.

Briesmeister, J. F. (1986), MCNP: A general Monte Carlo *N*-particle code, *Rep. LA-7396-M*, Los Alamos Natl. Lab., Los Alamos, N. M.

Cook, W. R., et al. (1993), PET: A proton/electron telescope for studies of magnetospheric, solar, and galactic particles, *IEEE Trans. Geosci. Remote Sens.*, *31*, 565–570.

Dean, A. J., A. J. Bird, N. Diallo, C. Ferguson, J. J. Lockley, S. E. Shaw, M. J. Westmore, and D. R. Willis (2003), The modeling of background noise in astronomical gamma ray telescopes, *Space Sci. Rev.*, *105*, 285–376.

Drake, D. M., T. E. Cayton, P. R. Higbie, D. K. McDaniels, R. C. Reedy, R. D. Belian, S. A. Walker, L. K. Cope, E. Noveroske, and C. L. Baca (1993), Experimental evaluation of the BDD-I dosimeter for the Global Positioning System, *Nucl. Instrum. Methods Phys. Res., Sect. A*, *333*, 571–588.

Fan, W. C., C. R. Drumm, S. B. Roeske, and G. J. Scrivner (1996), Shielding considerations for satellite microelectronics, *IEEE Trans. Nucl. Sci.*, *43*, 2790–2796.

Grupen, C. (1996), *Particle Detectors*, Cambridge Univ. Press, New York.

Jun, I., J. M. Ratliff, H. B. Garrett, and R. W. McEntire (2002), Monte Carlo simulations of the Galileo energetic particle detector, *Nucl. Instrum. Methods Phys. Res., Sect. A*, *490*, 465–475.

Rosen, A., and N. L. Sanders (1968), Pegasus 1: Observations of the temporal behavior of the inner zone electrons, 1965–1966, *J. Geophys. Res.*, *73*, 1019–1033.

Sauer, H. H. (1978), Atlas of polar cap energetic particle observations, volume I, TIROS-N, 1 January 1979 to 28 February 1981, *Data Rep. ERL-SEL-3*, Natl. Oceanic and Atmos. Admin., Silver Spring, Md.

Tuszewski, M., T. E. Cayton, and J. C. Ingraham (2002), A new numerical technique to design satellite energetic electron detectors, *Nucl. Instrum. Methods Phys. Res., Sect. A*, *482*, 653–666.

Vampola, A. L. (1998), Measuring energetic electrons: What works and what doesn't, in *Measurement Techniques in Space Plasmas: Particles, Geophys. Monogr. Ser.*, vol. 102, pp. 339–355, AGU, Washington, D. C.

Vampola, A. L., J. V. Osborne, and B. M. Johnson (1992), CREES magnetic electron spectrometer AFGL-701-5A (MEA), *J. Spacecr. Rockets*, *29*, 592–594.

———————————
T. E. Cayton, J. C. Ingraham, R. M. Kippen, and M. Tuszewski, Group ISR-2, Mail Stop B244, Los Alamos National Laboratory, Los Alamos, NM 87545, USA. (tcayton@lanl.gov; cingraham@lanl.gov; mkippen@lanl.gov; mgtu@lanl.gov)